STRUCTURE OF CHEMICAL COMPOUNDS, QUANTUM CHEMISTRY, AND SPECTROSCOPY

Ab initio Calculations of the Lowest $^1\Sigma_g^+$ States of the Na$_2$ Dimer

S. O. Adamson[a, *], **D. D. Kharlampidi**[b], **Sh. Sh. Nabiev**[c], **G. V. Golubkov**[a, c],
Yu. A. Dyakov[a, d], **and M. G. Golubkova**[a]

[a] *Semenov Federal Research Center for Chemical Physics, Russian Academy of Sciences, Moscow, 119991 Russia*
[b] *Moscow State Pedagogical University, Institute of Biology and Chemistry, Department of General Chemistry, Moscow, 119435 Russia*
[c] *National Research Center Kurchatov Institute, Moscow, 123182 Russia*
[d] *Academia Sinica, Taipei, 11529 Taiwan*
*e-mail: sergey.o.adamson@gmail.com
Received April 16, 2019; revised June 26, 2019; accepted July 22, 2019

Abstract—The ground and 10 lowest excited $^1\Sigma_g^+$ adiabatic electronic states of the Na$_2$ dimer are calculated using the pseudopotential method. The use of the basis [$7s6p5d4f$] of atomic orbitals makes it possible to extend the range of available internuclear distances up to 1.7−50 Å. It is found that the theoretical values of the T_e and D_e constants are in a good agreement with the experimental ones. Herein you will find the sample calculations of the radial non-adiabatic coupling matrix elements enable to transform the basis of the adiabatic states to quasidiabatic one. It is found also that the Le Roy modified radius scales down the left boundary of an asymptotic range for the electronic state with the $(3s + 5p)$ dissociation limit and for the higher states.

1. INTRODUCTION

We are witnessing the appearance of a new field of science: the radio-chemical physics of the atmosphere whose aim is the investigation of radio waves propagation at 60−110 km altitudes [1−3]. This field features a number of scientific and technical applications, including positioning problems in the global navigation satellite systems (GNSS) [4, 5]. The main role in the radio-chemical physics of the atmosphere is assigned to the processes of l-mixing, dissociative recombination, and associative ionization and exchange, passing through the formation of intermediate highly excited (Rydberg) states of diatomic molecules, which determine the parameters of a non-equilibrium atmospheric plasma [6]. Before calculating the cross sections for the above processes, we need to take into account the contribution from the long-range Rydberg states localized in the region from $5R_e$ to $15R_e$, where R_e is the equilibrium internuclear distance of the ground electronic state. Therefore, to test and correct theoretical approaches, it makes sense to consider a well-studied system, for example, the Na$_2$ dimer [7].

Sodium dimer (Na$_2$) is one of the few diatomic molecules whose absorption and emission spectra were repeatedly investigated experimentally and theoretically in the last century [7−10]. Theoretical studies of the Na$_2$ were started in the second half of 1960s with

the calculations of equilibrium internuclear distance and dissociation energy of the ground electronic state [11−13]. The growth of computing power made possible the calculations of excited electronic states correlated with I−III dissociation limits [14−17], X→A and X→B transition moments, and lifetimes of excited rovibrational states [18−21].

A brief review of experimental and theoretical studies published before 1982 is presented in article [8]. Of the later studies, calculations of potential energy curves (PEC) for the excited electronic states [22−30], long-range potentials [31−36], as well as dipole transition moments and the lifetimes of excited rovibrational states [10, 37, 38] should be mentioned.

The reason for the interest to the excited electronic states of Na$_2$ are significant differences in their optical properties and non-uniformity of the vibrational and rotational energy contributions for the excited rovibrational states assigned to the same observed excited electronic state [10, 37, 38]. This feature of the molecule can be explained by the resonance (non-stationarity) nature of the excited rovibrational states, arising due to their delocalization in neighboring electronic states. Whereby the non-uniformity of the rovibrational states properties is associated with the complex behavior of adiabatic potential curves (several minima, potential barriers, avoided-crossings, etc.) uniting the

fragments of the covalent and ionic $(M^+ + M^-)$ diabatic states [37, 38].

At the moment, 83 adiabatic electronic states of the Na_2 are calculated in the range ~5—40 a.u. (2.6—21.2 Å) with high accuracy, including the $(1-11)^1\Sigma_g^+$ states correlating with dissociation limits below $Na^+(^1S) + Na^-(^1S)$ limit [28, 29, 37]. Despite the large size of the internuclear distances range, its left boundary does not allow the repulsive branches of the adiabatic potential curves to reach the energy values of the corresponding dissociation energies. The right boundary includes only the avoided-crossing of $(5-6)^1\Sigma_g^+$ states. Unfortunately, this range is not sufficient for calculating the properties of the rovibrational states with energies greater than the avoided-crossing energy of the $(5-6)^1\Sigma_g^+$ adiabatic potential curves.

This study creates the adiabatic potential energy curves of $(1-11)^1\Sigma_g^+$ states in a larger range of internuclear distances than those presented in previous work [28]. The method of the calculations is presented in the second part, and the third part contains the detailed analysis of the results of the article. The conclusion suggests the way forward in the further development of the theory as well as the main challenges.

2. THE CALCULATION METHOD

Non-empirical (ab initio) studies of the excited adiabatic electronic states of Na_2 were carried out previously using a multi-configuration self-consistent field (MC SCF) [16, 20], restricted configuration interaction (RCI) [15, 17, 22, 23], and full configuration interaction (FCI) methods [24, 28, 37, 38]. All computational techniques considered Na_2 as a two-electron system: atomic $[Na^+]$ cores were frozen in full-electron atomic orbital bases (AO) [16, 20] or replaced by effective core pseudopotentials (ECP) [15, 17, 22—24, 28, 37, 38].

The non-empirical pseudopotential created by Durand and Barthelat was the most successful of the proposed ECPs [39]. Its incorporation with the $(7s6p5d2f)/[6s5p4d2f]$ Gaussian-type basis set and the core polarization potential (CPP) [40] made it possible to achieve better agreement with the experimental results [28] in comparison with the calculations [23, 24]. For the correct reproduction of the ^2F $(4f)$ atomic state, this basis set was expanded later by diffuse f-type functions according to the $(3f)/[2f]$ contraction scheme [41, 42]. In this form, the AO basis set with the same parametrization of the ECP/CPP potentials was used in the excited states calculations of NaH [43], LiNa [44, 45], NaCs [46], NaAr [41], and $LiNa^+$ molecules [42, 47]. The two other AO bases sets constructed from the AO set [28] were used to calculate the electric dipole moments of heteronuclear alkali metal dimers [48] and in modeling the interaction of Na_2 with argon clusters [30].

The calculations of the excited $^{1,3}\Sigma^+$ states of NaH molecule were performed using the non-empirical ECP [49, 50] with the CPP potential [51, 52] and the valence AO basis $[7s6p3d1f]$ [53] for the Na atom. This approach provides the reproduction of the sodium $3s-5s$ excitation energies with a deviation from the subsequent experimental values about ~10 cm^{-1}, but it loses significant accuracy of the NaH ground state description in comparison with the above mentioned combination of ECP/CPP potentials [41, 42].

The results of the adiabatic electronic states calculations of Na_2 and NaH molecules suggest that the best agreement with experimental data is achieved by pseudopotential and AO basis [42]. However, for a Na_2 molecule at internuclear distances less than 2.4 Å (~4.5 a.u.), the minimal eigenvalue of the AO's overlap matrix is less than 10^{-6}, which indicates the appearance of a computational linear dependence. When the most diffuse p-type function with the exponent $\alpha_p = 0.0023$ is excluded from the AO set, the minimal eigenvalue of the overlap matrix increases approximately three times, but the accuracy of the sodium ^2P $(3p-5p)$ states calculations decreases. This problem can be solved by reoptimizing several diffuse p-type functions, remembering that the relations of their exponents are dangerously close (~2.49—2.52) and the optimization should lead to a computational linear dependence with a high probability. In this situation it is most reasonable to reoptimize the AO basis set completely.

The calculations were performed with the Na effective core pseudopotential [39], supplemented by $(7s6p5d4f)/[7s6p5d4f]$ AO basis set (Table 1). The core-valence electron correlation was taken into account using the core polarization potential with $\alpha_s = 0.9947$, $\rho_s = 0.9605$ a.u. [51, 52]. The sodium AO set optimization was started from the total energy minimization using the four s-type Gaussian functions, and then the exponents of the remaining functions were optimized in order to better reproduce the energies of the excited $3p-4f$ atomic states. Finally, the maximum deviation from the experimental excitation energies is about 11 cm^{-1} for the ^2D $(4d)$ state (Table 2). As in previous works [24, 28, 37, 38], the two-electron wave function of the Na_2 molecule was constructed in full configuration interaction approach (FCI). All calculations were performed with the MOLPRO program package [54].

To evaluate the parameters of the avoided-crossings between the adiabatic states, the ionic diabatic potential curve correlating with the $Na^+ + Na^-$ dissociation limit was constructed [29]. The sodium ionization potential of 41 449.45 cm^{-1} [55], electron affinity of 4419.32 cm^{-1} [56] and polarizabilities $\alpha(Na^+) = 0.998033$ a.u. [57], $\alpha(Na^-) = 1090.2$ a.u. [58], which

Table 1. AO basis set for sodium

AO	Exponent
s	2.662241, 0.853282, 0.273488, 0.087656, 0.028095, 0.009492, 0.002746
p	1.048871, 0.325736, 0.106338, 0.031416, 0.006500, 0.002500
d	0.314937, 0.065639, 0.022201, 0.009123, 0.003435
f	0.053883, 0.016108, 0.005857, 0.002130

Table 2. Excitation energies of the sodium atom (cm^{-1})

Electronic state	E_{exc}	ΔE_{exc}				
		[28][a]	[53]	[41]	[43, 47]	calculation[b]
^{2}S(3s)	0	0	0	0	0	0
^{2}P(3p)	16968	+1	+11	+1	+1	+7
^{2}S(4s)	25740	−19	+9	−2	−2	−9
^{2}D(3d)	29173	+1	−536	0	0	+1
^{2}P(4p)	30271	+3	+8	−1	−1	−1
^{2}S(5s)	33201	−10	+8	−6	−5	−8
^{2}D(4d)	34549	−7	–	−13	−13	−11
^{2}F(4f)	34587	−16	–	–	−25	−7
^{2}P(5p)	35042	−13	–	−14	–	−40
^{1}S$_0$(2p^6)	41450	+1	0	0	0	−1

E_{exc} is the experimental excitation energy [55], ΔE_{exc} — difference between the experimental and calculated excitation energy.
a) ECP calculations (Method A);
b) present work.

are in a good agreement with theoretical and experimental estimates [59, 60], were used to parametrize this curve.

3. RESULTS AND DISCUSSION

The combination of the ECP and CPP potentials with the [7s6p5d4f] sodium AO basis set allows to construct adiabatic potential curves of $(1-11)^1\Sigma_g^+$ states in the range of internuclear distances of 1.7–50 Å (Fig. 1). Lowering the left interval boundary by 0.9 Å with respect to [28] made it possible for the repulsive branches of the potential curves to reach the energies exceeding the $(3s + 5p)$ dissociation limit energy. The value of 50 Å for the right border of internuclear distances interval was adequate to detect the avoided-crossing of $(10-11)^1\Sigma_g^+$ states (Fig. 1). It was shown that the values of the electronic terms (T_e) and dissociation energies of (D_e) $(1-6)^1\Sigma_g^+$ states are in better agreement with the experimental ones than the results of the previous calculations [28]. The calculated values of the equilibrium internuclear distances (R_e) were smaller than the experimental ones by ~0.01 Å. A significant error in the calculated R_e values is most likely a consequence of the adiabatic approach, which does not take into account non-adiabatic and relativistic effects. Only the experimental T_e = 34587.58, 34976.59 cm^{-1} values are known for the higher lying $(7-8)^1\Sigma_g^+$ states [61], which are in satisfactory agreement with the calculated terms of these states. For states $(9-11)^1\Sigma_g^+$, the experimental T_e and D_e values are absent and the calculated ones diverge by 600–2000 cm^{-1} (Table 3).

In addition to molecular constants, the parameters of avoided-crossings of the adiabatic potential curves were calculated similarly to [65]. For $(1-6)^1\Sigma_g^+$ states the crossing point positions (R_c) turned out on 0.01–0.02 Å larger than the positions predicted for the Rydberg–Klein–Rees (RKR) potentials. For the same electronic states the crossing energy ($E_c(R_c)$) and the width ($\Delta E(R_c)$) values differ slightly from the experimental ones by 30–60 cm^{-1} (Table 4).
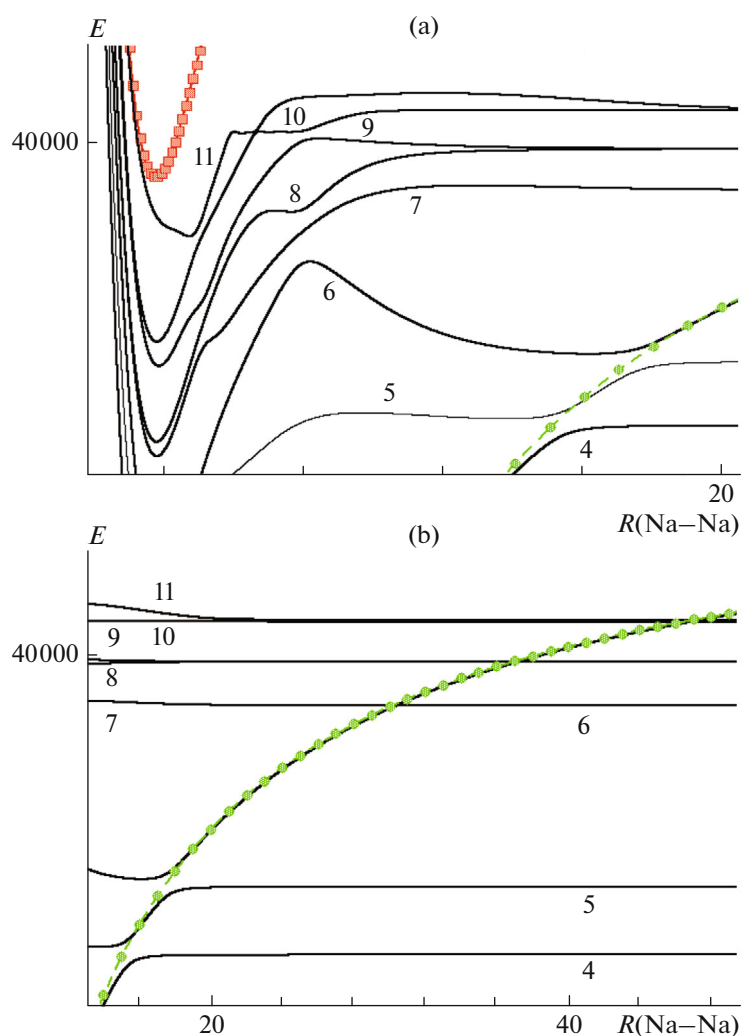
Fig. 1. Adiabatic electronic $(4-11)^1\Sigma_g^+$ states of Na_2 in the range 1.7−20.5 Å (a) and 13−50 Å (b). The dashed lines denote the ground state of the Na_2 ion (□) and the empirical diabatic ionic curve (●), and the solid lines indicate $^1\Sigma_g^+$ state of Na_2. The numbering of $^1\Sigma_g^+$ state curves corresponds to the nomenclature notation. The reference point of the energy scale is the position of the minimum energy of the ground electronic state (cm^{-1}).

The avoided-crossing regions in a system of $(6-11)^1\Sigma_g^+$ states are localized at small intervals of internuclear distances (~0.1−0.5 Å) and have small widths (~0.05−9 cm^{-1}). These features indicate that the calculations of the properties of excited rovibrational states require taking into account the non-adiabatic couplings. This problem can be solved by the transformation to the basis of quasidiabatic states with the subsequent solution for a system of coupled equations [69]. Because of the spatial localization of the avoided-crossings, it is necessary to examine the stability of the radial non-adiabatic coupling matrix elements (NACME) calculation (or overlap of adiabatic wave functions if the variational theory of effective Hamiltonian applied to construct quasidiabatic states

[69]) to the choice of the differentiation step size. The NACME calculations were performed with the two finite-difference approximations for the first derivatives of the electronic wave function at $R(Na-Na) = $ 11.25 Å. In the first approximation the derivative was replaced by an expression for the two-point right estimation (Method A). In the second, it was replaced by a two-point central difference (Method B). It was found that the differentiation step of 0.0001−0.000025 a.u. sufficient to calculate NACME values with an accuracy of five significant digits (Table 5). These results allow to conclude that the adiabatic $(6-11)^1\Sigma_g^+$ states can be included in a system of coupled equations for the nuclei motion after the transformation to the quasidiabatic states basis set.

Table 3. Molecular constants of the lowest electronic $^1\Sigma_g^+$ states

State	Limit	Experiment				Theory			
		R_e	T_e	D_e	source	R_e	T_e	D_e	source
$1^1\Sigma_g^+$	$3s + 3s$	3.080	0	6022	[62]	3.085	0	5892	[28][a]
						3.069	0	5987	PW
$2^1\Sigma_g^+$	$3s + 3p$	4.450	19338	3658	[63]	4.445	19349	3509	[28]
						4.446	19325	3623	PW
$3^1\Sigma_g^+$	$3s + 4s$	3.563	25692	6071	[63]	3.556	25615	6035	[28]
		3.569	25692	6070	[64, 65]	3.551	25662	6075	PW
$4^1\Sigma_g^+$	$3s + 3d$	4.073			[65]	4.069	28240	6825	[28]
		4.074	28327	6868[b]	[66]	4.061	28277	6883	PW
$5^1\Sigma_g^+$	$3s + 4p$	3.638	31770	4525	[67]	3.625	31700	4464	[28]
						3.626	31737	4522	PW
$6^1\Sigma_g^+$	$3s + 5s$	3.735	32563	6660	[36, 68]	3.710	32460	6643	[28]
						3.698	32506	6691	PW
$7^1\Sigma_g^+$	$3p + 3p$		34587		[61]	3.625	34572	5253	[28]
						3.614	34631	5271	PW
$8^1\Sigma_g^+$	$3p + 3p$		34977		[61]	3.625	35025	4801	[28]
						3.604	34876	5026	PW
$9^1\Sigma_g^+$	$3s + 4d$					3.598	34724	5539	[28]
						3.677	36176	4372	PW
$10^1\Sigma_g^+$	$3s + 4f$					3.577	35900	4416	[28]
						3.612	36590	3992	PW
$11^1\Sigma_g^+$	$3s + 5p$					3.577	36063	4693	[28]
						4.556	38398	2671[c]	PW

Equilibrium internuclear distances R_e are presented in Å, electronic terms T_e and dissociation energies D_e – in cm^{-1};
(a) reference [28]; presented data were obtained for 1−8 $^1\Sigma_g^+$ states by means of ECP/CPP calculations (Method A) and for other states − by model potential calculations (Method B);
(b) (3s+3d) dissociation energy was taken from reference [65];
(c) the dissociation energy estimated for the internuclear distance 95 Å;
(d) PW − present work.

Table 4. Parameters of the avoided-crossings of the adiabatic $^1\Sigma_g^+$ electronic states

n	Experiment[a]			Calculation[b]			R_{LR-m}[c]	R_d
	R_c	$\Delta E(R_c)$	$E_c(R_c)$	R_c	$\Delta E(R_c)$	$E_c(R_c)$		
1	5.289	14989.2	12441.2	5.282	15007.5	12412.6	9.2	–
2	7.557	5001.8	25459.1	7.529	5018.1	25400.7	13.6	7.1
3	11.259	1383.3	32038.4	11.240	1323.1	31977.1	16.5	10.9
4	15.457	414.8	35253.9	15.434	419.8	35208.5	19.4	15.1
5	17.633	425.5	36369.0	17.640	361.2	36305.1	25.5	17.5
6	–	–	–	30.429	9.223	39197.9	27.0	30.4
7	–	–	–	37.255	0.399	39901.9	18.0	37.6
8	–	–	–	37.256	0.223	39902.3	18.0	37.6
9	–	–	–	46.931	0.070	40547.7	34.2	46.9
10	–	–	–	47.581	0.046	40581.6	29.4	47.6

Notations are: n—is the number of the lowest adiabatic state ($n^1\Sigma_g^+$), R_c—internuclear distance corresponding the minimal energy difference between avoided-crossed adiabatic electronic states (Å), $\Delta E(R_c)$—the minimal energy difference between the avoided-crossed adiabatic electronic states (cm^{-1}), $E_c(R_c)$—energy of the avoided-crossing center (cm^{-1}), R_{LR-m}—the modified Le Roy radius (Å), R_d—the left asymptotic boundary in according to the estimation on the energy of the ionic diabatic state (Å). The minimum energy of the ground electronic state corresponds the zero energy (cm^{-1});
(a) obtained for the RKR-potentials, the references are the same as in Table 3;
(b) present calculations;
(c) obtained for the quantum defect from reference [71].

Table 5. Non-adiabatic coupling matrix elements calculated for internuclear distance $R(\mathrm{Na-Na}) = 11.25$ Å

δR	A			B		
	A_{21}	A_{32}	A_{43}	A_{21}	A_{32}	A_{43}
0.004	−0.134020	−0.050170	−0.207886	−0.134054	−0.049966	−0.207273
0.002	−0.134124	−0.049733	−0.206240	−0.134127	−0.049736	−0.206247
0.001	−0.134126	−0.049735	−0.206244	−0.134127	−0.049736	−0.206247
0.0005	−0.134127	−0.049736	−0.206245	−0.134127	−0.049736	−0.206247
0.00025	−0.134127	−0.049736	−0.206246	−0.134127	−0.049736	−0.206247

Method A is two-point right estimation, method B—central difference. Notation A_{nm} corresponds to matrix element $A_{nm} = \langle \psi_n | d/dR | \psi_m \rangle$, where ψ_n is the wavefunction of the adiabatic electronic state $n^1\Sigma_g^+$, R – internuclear distance (all values are in atomic units).

At large internuclear distances, an ab initio or RKR potentials can be extended by long-range (asymptotic) potentials, which form depends on the nature of the dissociating system. As it was shown for $(3-5)^1\Sigma_g^+$ states of Na$_2$ the left boundary of the asymptotic region can be estimated using the modified Le Roy radius (R_{LR-m}) [7, 70]. Comparing the R_{LR-m} and R_c values you can to see that the condition $R_c > R_{LR-m}$ is fulfilled for the avoided-crossings of $(6-7)^1\Sigma_g^+$ and higher states, i.e., the R_{LR-m} radius shifts the left asymptotic boundary to the smaller internuclear distances (Table 4). A more reasonable estimation can be obtained if the left asymptotic boundary considered as a point on the ionic diabatic curve with the energy equal to the dissociation energy of the electronic state (Table 4).

4. CONCLUSIONS

A new basis of valence atomic orbitals made it possible to refine the properties of the adiabatic electronic $(1-11)^1\Sigma_g^+$ states in a wide range of internuclear distances, including the vicinities of the avoided crossings. It was found that for $6^1\Sigma_g^+$ ($3s + 5p$ limit) and for higher electronic states, the use of the modified Le Roy radius with a view to estimate the left asymptotic boundary leads to errors. It was shown that the matrix elements of the radial non-adiabatic coupling can be calculated with a high accuracy. In future, it gives a

possibility to transform the adiabatic basis set to a quasidiabatic one.

The findings can help to calculate the cross section of the quenching process in the collision of Rydberg sodium atoms. In future, the similar calculations may be made for systems containing nitrogen and oxygen atoms. The cross sections and rate constants of the main processes that determine the parameters of a nonequilibrium atmospheric plasma strongly depend on the density of the neutral species [72−75].

FUNDING

REFERENCES

1. G. V. Golubkov, M. I. Manzhelii, and I. V. Karpov, Russ. J. Phys. Chem. B **5**, 406 (2011).
2. G. V. Golubkov, M. I. Manzhelii, and A. A. Lushnikov, Russ. J. Phys. Chem. B **8**, 604 (2014).
3. G. V. Golubkov, M. I. Manzhelii, A. A. Berlin, A. A. Lushnikov and L. V. Eppelbaum, Russ. J. Phys. Chem. B **12**, 725 (2018).
4. G. V. Golubkov, M. I. Manzhelii, A. A. Berlin, and A. A. Lushnikov, Russ. J. Phys. Chem. B **10**, 77 (2016).
5. G. V. Golubkov, M. G. Golubkov, and M. I. Manzhelii, Russ. J. Phys. Chem. B **8**, 103 (2014).
6. V. V. Kuverova, S. O. Adamson, A. A. Berlin, et al., Adv. Space Res. **64**, 1876 (2019).
7. W. C. Stwalley, J. Mol. Spectrosc. **330**, 14 (2016).
8. K. K. Verma, J. T. Bahns, A. R. Rajaei-Rizi, W. C. Stwalley, and W. T. Zemke, J. Chem. Phys. **78**, 3599 (1983).
9. K. M. Jones, E. Tiesinga, P. D. Lett, and P. S. Julienne, Rev. Mod. Phys. **78**, 483 (2006).
10. N. Jayasundara, R. B. Anunciado, E. Burgess, S. Ashman, and L. Hüwel, J. Chem. Phys. **150**, 064301 (2019).
11. L. Szasz and G. McGinn, J. Chem. Phys. **45**, 2898 (1966).
12. L. Szasz and G. McGinn, J. Chem. Phys. **48**, 2997 (1968).
13. L. Goodfriend, J. Mol. Spectrosc. **30**, 111 (1969).
14. A. C. Roach, J. Mol. Spectrosc. **43**, 27 (1972).
15. J. N. Bardsley, B. R. Junker, and D. W. Norcross, Chem. Phys. Lett. **37**, 502 (1976).
16. D. D. Konowalow, M. E. Rosenkrantz, and M. L. Olson, J. Chem. Phys. **72**, 2612 (1980).
17. A. Valance and Q. Nguyen Tuan, Phys. Lett. A **82**, 116 (1981).
18. W. J. Tango and R. N. Zare, J. Chem. Phys. **53**, 3094 (1970).
19. L. K. Lam, A. Gallagher, and M. M. Hessel, J. Chem. Phys. **66**, 3550 (1977).
20. W. J. Stevens, M. M. Hessel, P. J. Bertoncini, and A. C. Wahl, J. Chem. Phys. **66**, 1477 (1977).
21. D. D. Konowalow and P. S. Julienne, J. Chem. Phys. **72**, 5815 (1980).
22. G. H. Jeung, J. P. Malrieu, and J. P. Daudey, J. Chem. Phys. **77**, 3571 (1982).
23. G. Jeung, J. Phys. B: At., Mol. Phys. **16**, 4289 (1983).
24. G. H. Jeung, Phys. Rev. A **35**, 26 (1987).
25. A. Henriet and F. Masnou-Seeuws, J. Phys. B: At., Mol. Phys. **20**, 671 (1987).
26. A. Henriet and F. Masnou-Seeuws, J. Phys. B: At., Mol. Phys. **23**, 219 (1990).
27. A. Henriet, F. Masnou-Seeuws, and O. Dulieu, Z. Phys. D **18**, 287 (1991).
28. S. Magnier, Ph. Millie, O. Dulieu, and F. Masnou-Seeuws, J. Chem. Phys. **98**, 7113 (1993).
29. S. Magnier, M. Aubert-Frkon, O. Bouty, et al., J. Phys. B: At., Mol. Opt. Phys. **27**, 1723 (1994).
30. M. Gross and F. Spiegelmann, J. Chem. Phys. **108**, 4148 (1998).
31. R. F. Barrow, J. Verges, C. Effantin, K. Hussein, and J. d'Incan, Chem. Phys. Lett. **104**, 179 (1984).
32. F. Vigne-Maeder, Chem. Phys. **85**, 139 (1984).
33. B. Bussery and M. Aubert-Frecon, J. Mol. Spectrosc. **115**, 169 (1986).
34. M. Marinescu and A. Dalgarno, Phys. Rev. A **52**, 311 (1995).
35. M. Marinescu, Phys. Rev. A **56**, 4764 (1997).
36. T. Laue, P. Pellegrini, O. Dulieu, et al., Eur. Phys. J. D **26**, 173 (2003).
37. A. Sanli, B. Beser, J. R. Edwardson, et al., J. Chem. Phys. **143**, 104304 (2015).
38. A. Sanli, X. Pan, S. Magnier, et al., J. Chem. Phys. **147**, 204301 (2017).
39. D. Maynau and J. P. Daudey, Chem. Phys. Lett. **81**, 273 (1981).
40. M. Foucrault, Ph. Millie, and J. P. Daudey, J. Chem. Phys. **96**, 1257 (1992).
41. M. B. El Hadj Rhouma, H. Berriche, Z. B. Lakhdar, and F. Spiegelman, J. Chem. Phys. **116**, 1839 (2002).
42. H. Berriche, J. Mol. Struct.: THEOCHEM **663**, 101 (2003).
43. N. Khelifi, J. Russ. Laser Res. **29**, 274 (2008).
44. N. Mabrouk and H. Berriche, J. Phys. B: At., Mol. Opt. Phys. **41**, 155101 (2008).
45. https://doi.org/10.1080/00268976.2019.1605098
46. N. Mabrouk and H. Berriche, Russ. J. Phys. Chem. A **91**, 1475 (2017).
47. N. Khelifi, R. Dardouri, O. M. Al-Dossary, and B. Oujia, J. Russ. Laser Res. **30**, 172 (2009).
48. M. Aymar and O. Dulieu, J. Chem. Phys. **122**, 204302 (2005).
49. P. Fuentealba, H. Preuss, H. Stoll, and L. von Szentpaly, Chem. Phys. Lett. **89**, 418 (1982).
50. T. Leininger, A. Nicklass, W. Kuchle, et al., Chem. Phys. Lett. **255**, 274 (1996).
51. W. Müller, J. Flesch, and W. Meyer, J. Chem. Phys. **80**, 3297 (1984).
52. W. Müller and W. Meyer, J. Chem. Phys. **80**, 3311 (1984).

53. H. S. Lee, Y. S. Lee, and G. H. Jeung, Chem. Phys. Lett. **325**, 46 (2000).

54. H.-J. Werner, P. J. Knowles, G. Knizia, F. R. Manby, M. Schütz, et al., MOLPRO, Ver. 2010.1, a Package of ab initio Programs. http://www.molpro.net.

55. J. E. Sansonetti, J. Phys. Chem. Ref. Data **37**, 1659 (2008).

56. H. Hotop and W. C. Lineberger, J. Phys. Chem. Ref. Data **14**, 731 (1985).

57. L. G. Gray, X. Sun, and K. B. MacAdam, Phys. Rev. A **38**, 4985 (1988).

58. N. C. Pyper, C. G. Pike, and P. P. Edwards, J. Am. Chem. Soc. **115**, 1468 (1993).

59. M. Masili, S. Carlos, and J. J. De Groote, Phys. Rev. A **70**, 054501 (2004).

60. J. Mitroy, M. S. Safronova, and C. W. Clark, J. Phys. B: At., Mol. Opt. Phys. **43**, 202001 (2010).

61. A. J. Taylor, K. M. Jones, and A. L. Schawlow, J. Opt. Soc. Am. **73**, 994 (1983).

62. W. T. Zemke and W. C. Stwalley, J. Chem. Phys. **100**, 2661 (1994).

63. C. Effantin, J. d'Incan, A. J. Ross, R. F. Barrow, and J. Verges, J. Phys. B: At., Mol. Phys. **17**, 1515 (1984).

64. Chin-Chun Tsai, T.-J. Whang, J. T. Bahns, and W. C. Stwalley, J. Chem. Phys. **99**, 8480 (1993).

65. Chin-Chun Tsai, J. T. Bahns, H. Wang, T.-J. Whang, and W. C. Stwalley, J. Chem. Phys. **101**, 25 (1994).

66. H. Wang, T.-J. Whang, A. Lyyra, L. Li, and W. C. Stwalley, J. Chem. Phys. **94**, 4756 (1991).

67. Chin-Chun Tsai, J. T. Bahns, and W. C. Stwalley, J. Chem. Phys. **100**, 768 (1994).

68. Chin-Chun Tsai, J. T. Bahns, and W. C. Stwalley, J. Mol. Spectrosc. **167**, 429 (1994).

69. S. Jellali, H. Habli, L. Mejrissi, B. Oujia, and F. X. Gadea, J. Phys. Chem. A **123**, 544 (2019).

70. Ji Bing, Chin-Chun Tsai, and W. C. Stwalley, Chem. Phys. Lett. **236**, 242 (1995).

71. W. C. Martin, J. Opt. Soc. Am. **70**, 784 (1980).

72. G. V. Golubkov, G. K. Ivanov, E. M. Balashov, et al., J. Exp. Theor. Phys. **87**, 56 (1998).

73. G. V. Golubkov and G. K. Ivanov, Khim. Fiz. **22** (10), 25 (2003).

74. G. V. Golubkov, G. K. Ivanov, and M. G. Golubkov, Khim. Fiz. **24** (6), 3 (2005).

75. G. V. Golubkov, G. K. Ivanov, and M. G. Golubkov, Khim. Fiz. **24** (9), 3 (2005).